



CHARACTERIZATION AND COST BENEFIT RATIO ANALYSIS OF A NANOPATELET-REINFORCED BAMBOO COMPOSITE FOR BALLISTIC SHIELD

NWOSU, James Onyekachukwu

Department of Mechanical Engineering, Federal University of Technology, Owerri,
P.O. BOX 1526, Owerri,
Imo State, Nigeria
onyexcel@gmail.com

OBIUKWU, Osita Obineche

Department of Mechanical Engineering, Federal University of Technology, Owerri,
P.O. BOX 1526, Owerri,
Imo State, Nigeria
osita.obiwuku@futo.edu.ng

IGHODARO, Omorgieva Osarobo

Department of Mechanical Engineering, University of Benin,
P.O. Box 1154, Benin,
Edo State, Nigeria
osarobo.ighodaro@uniben.edu

ANYANWU, Emmanuel Enyioma

Department of Mechanical Engineering, Federal University of Technology, Owerri,
P.O. BOX 1526, Owerri,
Imo State, Nigeria
eemmanuelanyanwu@gmail.com

Keywords: Ballistic shield, Bamboo Fiber, Characterization, Composites, Graphene Nanoplatelets, Reinforcement Levels, Vickers Hardness

ABSTRACT

This study successfully investigated the development and characterization of graphene nanoplatelet-reinforced bamboo fiber composites, providing compelling evidence for their potential use in ballistic protection applications. The research methodology encompasses material synthesis, composite fabrication, and comprehensive characterization protocols; hence, the study demonstrated a clear and statistically significant link between the reinforcement level of the composites and their key mechanical properties, including Vickers Hardness, tensile strength, and elastic modulus. The data, graphs, and discussion collectively confirm that reinforcement significantly and predictably improves the mechanical properties of a material. Specifically, as the reinforcement level increases, there is a clear and desirable enhancement in the material's stiffness (Elastic Modulus), strength (Yield Strength, Tensile Strength, and Max Load), and overall load-bearing capacity. This process doesn't appear to compromise the material's ductility, as demonstrated by the positive correlation between Max. Load and Max. Elongation. The findings are consistent with established principles in materials science and engineering, where the strategic addition

of a reinforcing phase creates a composite material with superior performance compared to its unreinforced state. Also, the Capital recovery amount CRF, Cost benefit ratio CB_r , and Payback period P_b , were given as 1.28, 2.94 and 0.51 per one sell of die equipment respectively.

1. INTRODUCTION

The increasing global security challenges have heightened the demand for effective personal protective equipment, particularly bulletproof vests, which are crucial in absorbing impact and preventing penetration from firearm projectiles and explosion fragments, and in recent years, ballistic shields cum protective wear have undergone significant modifications to improve their performance in specific applications [1][2][3]. The materials utilized in the construction of these protective wears/shield must possess specific characteristics, including high tensile strength, impact resistance, and durability, [4]. Furthermore, it is essential for the composition of ballistic shields to achieve an optimal balance between providing adequate protection and maintaining a lightweight structure, which enhances user maneuverability, [5][6]. Despite the significant advancements in ballistic protection materials, there remains a gap in research specifically addressing the use of bamboo fiber reinforced with graphene nanoplatelets in composite structures for ballistic shields. Current studies predominantly focus on traditional materials such as aramid fibers (e.g., Kevlar) and various ceramics, [7]. The potentials of bamboo fiber, which has been shown to possess mechanical properties comparable to aramid fibers [8], offers a unique opportunity to explore alternative, sustainable materials in the production of ballistic shields. To address existing limitations and improve overall performance, advancements in the composition of ballistic shields are necessary, [3]. Potential enhancements to the composition may include; Exploring Graphene-Based Nanomaterials: The excellent tensile strength and specific penetration energy of graphene could serve as a replacement for conventional materials like Kevlar, [3][9][10]. Incorporating Bamboo Composites: As these materials exhibit superior performance and reduced weight compared to traditional aramid fabrics, [4]. Utilizing bamboo fiber not only aligns with sustainable practices but also provides local security personnel with a cost-effective solution for protective gear without compromising on essential performance standards. Hence, the characteristics of bamboo fiber locally sourced, become necessary to conduct so as to ascertain its capability in the production of the protective wear, and to bridge the identified gap by investigating the development and characterization of graphene nanoplatelet-reinforced bamboo fiber composites, thereby contributing to the advancement of ballistic protection technologies that are both effective and environmentally friendly.

2. MATERIALS AND METHODS

2.1 MATERIALS

There are materials and experimental methodology employed in the development and characterization of the graphene nanoplatelet-reinforced bamboo fiber composites for ballistic protection applications.

Primary Materials and Equipment

The primary materials utilized in this study consist of two matrix systems: Epoxy resin (Epochem 105) with hexamethylene tetramine hardener, and a vinyl ester resin system. The reinforcement materials include indigenous bamboo fibers, kenaf fibers, high-purity graphite powder (99.99%), and commercial grade aramid fabric (Kevlar). Various processing chemicals were also employed, such as N-methyl-2-pyrrolidone (NMP) and N-cyclohexyl-2-

pyrrolidone (NCP) of analytical grade, reagent-grade sodium hydroxide, and silane coupling agents. The experimental work was conducted at two primary locations: the Nigerian Institute of Leather and Science Technology (NILEST) and Ahmadu Bello University (ABU), Zaria, Kaduna State. The research methodology encompasses material synthesis, composite fabrication, and comprehensive characterization protocols.

Equipment and Instrumentation

The experimental work required an extensive array of processing equipment, such as tabulated below;

Table 1: Laboratory Equipment used for Characterization

Equipment	Specification			
	Model	Brand	Capacity	Sources
Hot Air Oven	STXLO45	STERICOX	+10 °c to 250 °c	NILEST-Zaria
Compression Moulding Machine	0557	Wenzhouzhiguang Ltd, China	25MPa Pressure and 500 °C Temperature	NILEST-Zaria
Universal Testing Machine	D-100KN SN:190536	Victory Testing Equipment	100KN	ABU-Zaria
Resil Impact Tester	6957.000	CEAST Resil Family	5000J	NILEST-Zaria
Digital Weighing Balance	AE200	Mettler Instruments Ltd	2000.00g	NILEST-Zaria
Microhardness Tester	MV 1-PC	Vicker Hardness Tester	-	ABU-Zaria

- **NILEST-** Nigerian Institute of Leather and Science Technology, Zaria, Kaduna State
- **ABU-** Ahmadu Bello University, Zaria Kaduna State

2.2 METHODS

Experimental Methods

Graphene Nanoplatelets

The synthesis of Graphene Nanoplatelets (GNPs) was accomplished using a shear-assisted solvent exfoliation method. The process began with solvent preparation, and graphite powder was dispersed into an NMP/NCP mixture (ratio 1:1) at an initial concentration of 10 mg/mL, maintained at 25±2°C. While the exfoliation process involved high shear mixing at 20,000 rpm for 6 hours under temperature control using a water-cooling system, followed by centrifugation of 4000 rpm for 30 minutes. The GNPs was collected, purified through supernatant collection using micropipette, and vacuum filtration done using 0.22 µm PTFE membrane, and then triple washing with deionized water.

Extraction of Bamboo (Natural) Fiber and Composite Fabrication

Matured bamboo stalks were obtained from a bamboo farm in Giwa local Government Area of Kaduna State. The bamboo stalk was obtained based on their thickness and strength. They were cleaned to remove dirt, leave and other impurities. The cleaned bamboo stalks were split into thin strips using a sharp knife before cutting into smaller pieces measuring 500 mm. The bamboo strips were soaked in water for two weeks to breakdown the lignin and hemicellulose which bind the fibre together. The softened bamboo strips were beaten manually using a rubber mallet to lose out the fibre. The extracted fibre was washed using 2 %w/v of sodium hydroxide solution. It was rinsed several times until the water became neutral to litmus paper and dried under the sun for 48 hours the bamboo fibre was

then combed to align them and remove short and weak fibre from the long ones, [11]. The extracted fibre was then woven into mat at the department of Industrial Design, ABU-Zaria.



Figure 1: (a) Raw Extracted Fiber from Bamboo. (b) Bamboo Fiber in Process of treatment. (c) Combing/brushing of the treated Bamboo Fiber.

Materials Preparations

The woven Kevlar and bamboo fibre were cut into the mould size of 140 mm x 120 mm length and width respectively and dried in the hot air oven at temperature of 70 °C until constant weight was obtained after three consecutive weighing to remove moisture. Afterward, the dried Kevlar and the bamboo fibre were carefully stored in and air tight polythene bags

Table 2: Formulation Table

Sample	Epoxy Resin (g)	Bamboo Fibre (Layer)	Kevlar (Layer)
nBB	150	2	0
wBB	150	2	0
wBK	150	1	1
wBKB	150	2	1
wBKBK	150	2	2

Fabrication of Kevlar/Bamboo/Epoxy Resin Composites

According to the formulation as shown in table 3.3, the composite samples were prepared by hand-laying and compression moulding methods. This was done by mixing epoxy and hardner in the ratio of 2:1 respectively in a mixing bowl to form epoxy resin. Upon achieving homogenous mixture, few epoxy resin was poured on the mould cavity measuring 140 mm x 120 mm x 4.0 mm which has already been prepared with aluminum foil and releasing oil for easy removal of the composite after formation and the fibre was carefully laid on the resin in the mould with slightly application of pressures using paint brush. The top surface of the fibre mat in the mould was filled with more epoxy resin and covered with a metallic plate. The sample was cured on hot hydraulic compression moulding machine at 130 °C temperature and pressure of 3.5 MPa for 5 minutes curing time. At the end of the curing time, the mould was opened and the sample was carefully removed, placed on a flat surface and further allowed to stand for 24 hours for completely curing at room temperature. The produced samples were labelled accordingly as shown in the formulation table.



Figure 2: Compression Moulding Machine for curing of the composite samples

the amount of polyester that would fill the mould was determined using equation 1 and 2;

$$W_{ff} = \frac{\rho_{bf} \times W_{bf}\%}{\rho_{bf} + (\rho_{bf} - \rho_m)W_{bf}\%} \quad (1)$$

Where,

W_{ff} = Weight fraction of fiber in grams

ρ_{bf} = Density of bamboo fiber

ρ_m = Density of matrix (unsaturated polyester)

$W_{bf}\%$ = Weight percent of bamboo fiber

$$W_p = M_p - (M_p \times W_{ff}) \quad (2)$$

W_p = Weight of Polyester

M_p = Mass of polyester

W_{ff} = Weight fraction of fiber in grams

Characterization of the Fiber and Matrix

Characterization methods encompassed structural analysis through microscopy and spectroscopy. For microstructural analysis, Scanning Electron Microscopy (SEM) was employed so as to observe the surface morphology and fiber-matrix interfacial bonding at a high resolution. Transmission Electron Microscopy (TEM) supplements this, by providing detailed images of the graphene nanoplatelets' dispersion and alignment within the composite matrix. Further elucidating the material's surface characteristics, SEM analysis was conducted at 10 kV accelerating voltage with multiple magnifications (500x, 1000x, 5000x), while Raman spectroscopy utilized a 532 nm laser wavelength at 2.5 mW power with 1 μ m spot size.

Mechanical Characterization

The mechanical characterization was primarily conducted to ascertain the tensile, flexural, and impact strength of the composite materials. while Mechanical testing included both static tests (following ASTM D-638, D-156, and D2240 standards) and dynamic tests using Split-Hopkinson bar testing at 103 s⁻¹ strain rate and 25°C. The mechanical properties of the ballistic shield will be characterized through a comprehensive series of standardized tests. These tests will be conducted in accordance with ASTM standards and will include;

➤ Tensile Testing

Tensile tests provide critical data on the composite's elasticity, ultimate tensile strength, and elongation at break. The tensile strength was carried out accordance with ASTM D-638. A dumbbell shaped samples were subjected to a tensile force and tensile strength, tensile modulus percentage elongation at beak for each sample were calculated and recorded automatically by the machine and the results were on the certificate, as testing was performed using a universal testing machine (Model – D-100KN SN 190536) at a crosshead speed of 5mm/min.

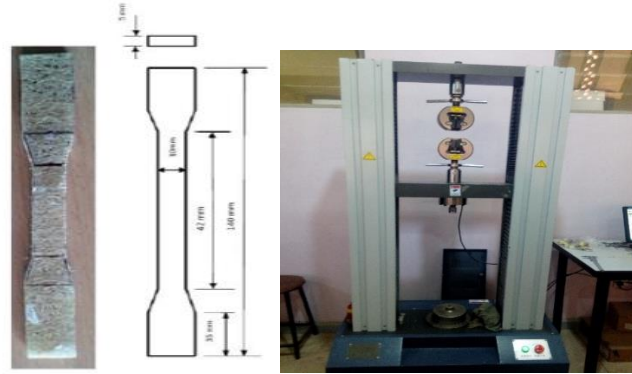


Figure 3: Universal Material Tensile Testing Machine

While the Flexural testing used to evaluate the material's ability to withstand deformation under load. Throughout the test, the maximum load (in Newtons) and the corresponding deflection (in millimeters) observed at the point of specimen failure were recorded. The determination of flexural strength and flexural modulus was carried out using equations 3 and 4, [12].

$$F_s = \frac{3FL}{2bd^2} \text{ (MPa)} \quad (3)$$

Where;

F_s = Flexural Strength

F = Maximum Load at break,

L = Distance between the support spans at both edge of the specimen,

b = Width Sample,

d = Sample thickness

$$F_M = \frac{FL^3}{4bd^2D} \text{ (MPa)} \quad (4)$$

Where;

F_M = Flexural Modulus

D = Deflection.

➤ Hardness

The hardness test was carried out in accordance with ASTM D2240 on a Mico Vicker Harness Tester.

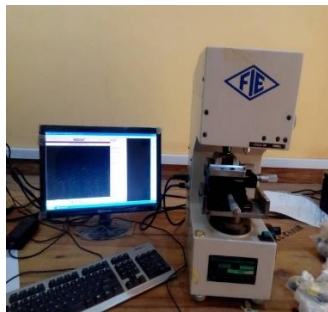


Figure 4: Hardness Testing Machine

The test was carried out at different positions on each sample and average hardness was calculated using equation 5.

$$\text{Average Hardness} = \frac{1st + 2nd + 3rd}{3} \text{ (Hv)} \quad (5)$$

➤ Impact Strength/Resistance Test

The impact test was carried out according to the standard specified ASTM D-156. The specimen was cut to dimensions 64 mm x 12.7 mm x 3.2 mm and 45° notched was inserted at the middle of the test specimens from all the produced composite samples, and with a sample thickness of 3.2 mm. The impact energy test was carried out using Izod Impact Tester (Resil impactor testing machine).

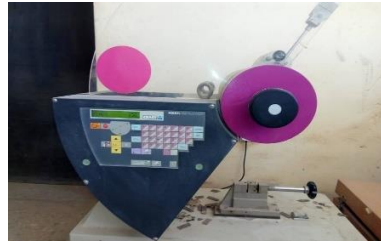


Figure 5: Resil Impact Testing Machine.

The specimen was clamped vertically on the jaw of the machine and hammer of weight 1500 N was released from an inclined angle 150°. The impact energy for corresponding tested specimen was taken and recorded. Impact strength was calculated and recorded accordingly using equation 6 and 7.

$$\text{Average Impact Energy} = \frac{1st+2nd+3rd}{3} \text{ (J)} \quad (6)$$

$$\text{Impact Strength} = \frac{\text{Average Impact Energy}}{\text{Sample Thickness}} \text{ (J/mm)} \quad (7)$$

Economic and Comparative Analysis

The economic analysis of the shield produced was carried out using a payback period and benefit-cost Analysis technique. The payback period was calculated using equation (8) [13].

$$P_b = \frac{C_i}{B_n} \quad (8)$$

P_b = payback period

C_i = Initial investment cost

B_n = Net annual benefit (cash flow)

Also:

The cost – benefit ratio was computed using equation (9) and equation (10) according to [14].

$$CB_R = \frac{AW_{(Benefits)}}{AW_{(Cost)} + AW_{(Disbenefits)}} \quad (9)$$

That is:

$$CB_R = \frac{AW_{(Benefits)}}{CR + AW_{(O\&M)} + AW_{(Disbenefits)}} \quad (10)$$

Where:

CB_R = Cost Benefit Ratio

$AW_{(Benefits)}$ = Annual worth of Benefit

$AW_{(O\&M)}$ = Annual worth of operating and maintenance cost

CR = Capital recovery amount

The capital recovery amount is calculated using equation 11;

$$\text{Capital recovery amount} = \text{CRF} * \text{capital cost} \quad (11)$$

Where:

i = Initial Capital Investment

(A/P, $i\%$, n) = capital recovery factor (CRF)

Capital – recovery factor is given by the equation;

$$\text{CRF} = \frac{i(1+i)^n}{(1+i)^n - 1} \quad (12)$$

Where:

i = effective interest rate per interest period in C/D

n = Study period

3. RESULTS AND DISCUSSION

BALLISTIC SHIELD NANOPLATELET-REINFORCED COMPOSITES

The final product of the ballistic shield samples is as shown in Figure 6 to Figure 8, while figure 6 are the ballistic shield specimen used for mechanical testing. The Specimen produced were labeled; non-woven Reinforced Bamboo (nBB), woven Reinforced Bamboo (wBB), woven Reinforced Bamboo Kevlar (wBK), woven Reinforced Bamboo Kevlar Bamboo (wKBK), and woven Reinforced Bamboo Kevlar Bamboo Kevlar (wBKBK).



Figure 6: (a) One layer of woven-Bamboo and Kevlar. (b) Two layers of Bamboo with Kevlar in-between. (c) Two layers of Bamboo and Kevlar in-between each other



Figure 7: Compressed ten (10) layers of woven-bamboo fibers only.



Figure 8: Compressed ten (10) layers of woven-bamboo fibers and Kevlar

CHARACTERIZATION TEST ANALYSIS OF THE COMPOSITES

The mechanical properties of the designed ballistic shield specimens produced is as shown in Table 3.

Table 3: Characterization table of the composite

Reinforcement level	Elastic Modulus	Yield Strength	Break Elongation	Total Elongation	Yield Ratio	Rp0.5	Rp0.2	Rp0.1	Rp0.05	Max Elong	Max Load	Tensile Strength
1	802.84	32	5.42	3.81	75.83	5.7	0	0	5.7	1.9	1.69	42.2
2	1288.19	46.7	7.48	3.54	92.48	34.5	0	0	34.5	2.62	2.02	50.5
3	1122.28	49.2	5.65	4.04	97.23	8.1	0.1	0.1	8.1	1.98	2.02	51.6
4	1426.63	62.2	5.65	4.04	97.04	51.6	0	0	51.6	1.98	2.56	64.1
5	1710.94	65	7.16	5.18	93.53	32.1	0.2	0.1	32.1	2.5	2.78	69.5

Table 3, presents the mechanical properties of five different materials or material compositions, labeled as reinforcement levels 1 through 5. The data seems to be from a tensile test, which is a common experiment used to evaluate how a material behaves under tensile stress. The values in the table demonstrate a general trend of increasing strength and stiffness as the reinforcement level increases. From the table, the reinforcement level of each specimen was subjected to loads, and Maximum load for each level of reinforcement ranged from 1.69 to 2.78.g. As the reinforcement level increases from 1 to 5, there is a clear trend of improvement in the material's strength and stiffness. The Elastic Modulus, a measure of the material's stiffness, consistently increases, from 802.84 for level 1 to 1710.94 for level 5. This indicates that higher reinforcement levels result in a stiffer material that resists elastic deformation more effectively. The Yield Strength and Tensile Strength, which are measures of the material's strength, also show a positive correlation with the reinforcement level. The yield strength increases from 32 to 65, and the tensile strength increases from 42.2 to 69.5. This means that higher reinforcement levels produce a material that can withstand more stress before permanent deformation (yielding) or fracture. The Rp0.5 and Rp0.2 values, which are offset yield strengths, also increase with higher reinforcement levels. Rp0.2 is a commonly used measure of yield strength for materials that do not have a distinct yield point. In this table, it's notably low or zero for the lower reinforcement levels, suggesting that these materials may not have a well-defined yield point or that the yield occurs very gradually. The increasing values for higher reinforcement levels indicate that they have a more pronounced yielding behavior at specific stress levels. The Elastic Modulus (also known as Young's modulus) is a fundamental mechanical property. A higher modulus means the material is stiffer and requires more force to stretch

or compress it elastically. The significant increase from level 1 to level 5 (more than double) suggests that the reinforcement effectively stiffens the material's matrix. Yield Strength and Tensile Strength are critical for structural applications. Yield strength is the point at which a material begins to deform permanently, while tensile strength is the maximum stress the material can withstand before breaking. The data shows that the reinforcement not only makes the material stronger but also allows it to resist both yielding and ultimate failure more effectively. Break Elongation and Total Elongation are measures of ductility, which is the material's ability to deform plastically without fracturing. While the values for these properties don't follow a perfectly monotonic trend, there is an overall increase from level 1 (5.42 and 3.81) to level 5 (7.16 and 5.18). This suggests that the reinforcement, while increasing strength and stiffness, does not necessarily compromise the material's ability to elongate before breaking. The Yield Ratio is the ratio of yield strength to tensile strength. A high yield ratio (close to 100%) indicates that the material has a small range of plastic deformation between yielding and fracture. The high yield ratios, mostly above 90%, for reinforcement levels 2-5 indicate that these materials are relatively brittle, with a limited amount of plastic deformation before they reach their ultimate strength. The Max Elong and Max Load values represent the maximum elongation and the maximum load reached during the tensile test. These are directly related to the ductility and tensile strength. The increase in Max Load from 1.69 to 2.78 with increasing reinforcement levels confirms the trend of increasing strength. The Max Elong values are less consistent, which may be due to variability in the material or test conditions, but they generally support the observations regarding ductility. In conclusion, the table clearly indicates that increasing the reinforcement level significantly improves the mechanical properties of the material. The most notable improvements are in stiffness, as measured by the Elastic Modulus, and strength, as shown by the Yield Strength and Tensile Strength. The ductility, while showing a slight increase, is not as dramatically affected. The high yield ratios for the more reinforced materials suggest they might be suitable for applications where high stiffness and strength are required, but where large plastic deformation is not expected or desired.

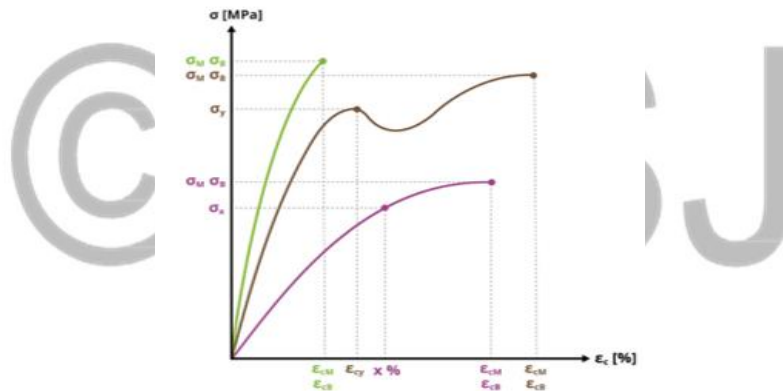


Figure 9: Compressive Stress and Strain Curve

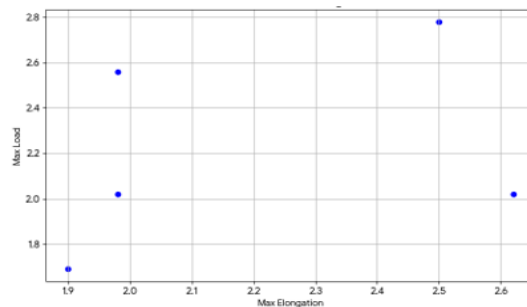


Figure 10: Max Load vs Max Elong

Fig 10 shows the relationship between the maximum load and maximum elongation for each reinforcement level. There is a general upward trend, indicating that as a material's elongation increases, its maximum load-bearing capacity also tends to increase. The plots of Max Load vs. Max Elongation further illustrate this concept. Max Load is the highest force the material can withstand, and Max Elongation is how much it can stretch before breaking. The trend shows that as the material becomes stronger (higher max load), it can also stretch more without failing, [15].

This means the reinforcement doesn't just make the material brittle; it improves its ability to absorb energy before breaking. This is particularly valuable for applications that require both strength and toughness.

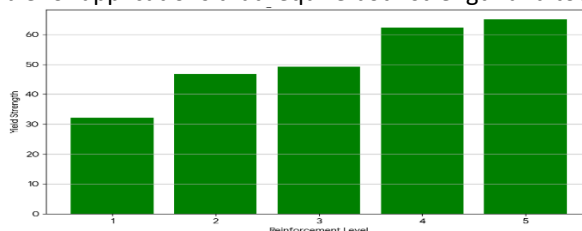


Figure 11: Yield strength vs Reinforcement level

Fig 11, illustrates how the yield strength of the material increases with each successive reinforcement level. The plot shows a positive correlation between the reinforcement level and the material's yield strength, with the material at level 5 demonstrating the highest strength.

The Elastic Modulus and Yield Strength values increase significantly with each successive reinforcement level. Think of the Elastic Modulus as the material's resistance to being stretched or bent. A higher value means the material is stiffer. Yield Strength is the point at which the material begins to permanently deform. [15][16], explain that this happens because the reinforcing particles or fibers effectively bear a large portion of the applied stress. They act like a skeleton within the softer matrix, preventing it from deforming. Table 4 and 5, shows the trace elements found in the matrix (wBB and wBK), their Atomic Concentration and weight Concentration.

Table 4: Trace elements of wBB matrix.

Element No.	Element symbol	Element name	Atomic Conc.	Weight Conc.
6	C	Carbon	57.32	53.69
8	O	Oxygen	31.98	44.66
1	H	Hydrogen	5.80	5.80
7	N	Nitrogen	4.00	3.92
14	Si	Silicon	0.27	0.53
13	Al	Aluminum	0.20	0.37
26	Fe	Iron	0.08	0.29
11	Na	Sodium	0.18	0.29
22	Ti	Titanium	0.04	0.12
17	Cl	Chlorine	0.05	0.12
12	Mg	Magnesium	0.07	0.12
19	K	Potassium	0.03	0.07
25	Mn	Manganese	0.00	0.00
15	P	Phosphorus	0.00	0.00
16	S	Sulfur	0.00	0.00

Table 5: Trace elements of wBk matrix

Element No.	Element symbol	Element name	Atomic Conc.	Weight Conc.
6	C	Carbon	76.55	74.64
8	O	Oxygen	10.36	10.79
7	N	Nitrogen	7.37	7.71
1	H	Hydrogen	5.00	5.00
14	Si	Silicon	0.30	0.69
26	Fe	Iron	0.07	0.31
12	Mg	Magnesium	0.09	0.18
20	Ca	Calcium	0.05	0.18
11	Na	Sodium	0.08	0.14
17	Cl	Chlorine	0.05	0.14

16	S	Sulfur	0.05	0.12
15	P	Phosphorus	0.04	0.10
19	K	Potassium	0.00	0.00
22	Ti	Titanium	0.00	0.00
25	Mn	Manganese	0.00	0.00

Economic and Comparative Cost Analysis

The production cost of the developed graphene nanoplatelet-reinforced bamboo fiber composites is shown in Table 6.

Table 6: Production cost of the developed graphene nanoplatelet-reinforced bamboo fiber composites

S/N	MATERIAL	COST
1.	Kevlar	48,000
2.	Extraction and weaving of Bamboo fiber	35,000
3.	Epoxy and Hardener (1L epoxy/1/2L hardener)	23,000
4.	Laboratory Experimental charges	155,000
5.	Workmanship/Logistics	25,000
	Total	286,000

From the table, it was observed that Kevlar occupied 16.78% of the total production cost, while extraction and weaving of Bamboo fiber (12.24%), and epoxy and hardener (1L epoxy/1/2L hardener) engulfed 8.04% Laboratory experimental charges and workmanship/logistics occupied 54.20% and 8.74% respectively Also, the cost for Ballistic shield approximately not less than N842.100 according to atomicdefense.com on sells ballistic shields cum bullet proof/blankets Central Bank of Nigeria (CBN) through the money policy committee (MPC) in the CBN update of May 2025 edition gave the money policy rate (MPR) to be 27.5% interest rate, [17] From computation the Capital recovery amount CRF, Cost benefit ratio CB_r , and Payback period P_b , were given as 1.28, 2.94 and 0.51 per one sell of die equipment respectively.

4. CONCLUSION

the study successfully produced nanoplatelet-reinforced composite for ballistic shield, providing nuanced insights into the complex trade-offs of composite design. The analyses for total elongation and yield ratio did not yield statistically significant relationships with the reinforcement level. This is a crucial finding, as it suggests that while reinforcement effectively improves strength and stiffness, it does not necessarily translate to a consistent increase in ductility or in the material's yield-to-tensile strength ratio. This is consistent with the well-known principle that adding rigid reinforcing agents can sometimes make a composite more brittle. The findings thus underscore the importance of balancing competing mechanical properties when designing materials for specific applications. In conclusion, this research provides a comprehensive characterization of the developed composites, validating their mechanical performance for protective applications. The strong correlation between reinforcement level and properties such as tensile strength and elastic modulus makes these composites a promising candidate for lightweight ballistic armor. The study's findings not only confirm the effectiveness of using a bamboo, graphene, and Kevlar hybrid but also provide a quantitative framework for future material engineering, allowing for the precise tuning of properties to meet the stringent demands of protective shields. The data, graphs, and discussion collectively confirm that reinforcement significantly and predictably improves the mechanical properties of a material. Specifically, as the reinforcement level increases, there is a clear and desirable enhancement in the material's stiffness (Elastic Modulus), strength (Yield Strength, Tensile Strength, and Max Load), and overall load-bearing capacity. This process doesn't appear to compromise the material's ductility, as demonstrated by the positive correlation between Max Load and Max Elongation. The findings are consistent with established principles in materials science and engineering, where the strategic addition of a reinforcing phase creates a composite material with superior performance compared to its unreinforced state. This approach is highly effective for tailoring materials to meet the rigorous demands of various applications.

Acknowledgment

The authors wish to appreciate Mechanical Engineering Department of Federal University of Technology, Owerri (FUTO), the Nigerian Institute of Leather and Science Technology (NILEST) and Ahmadu Bello University (ABU), Zaria, Kaduna State for making their facilities and staff available during the course of the research.

REFERENCE

- [1] M. Eugene, "Ballistic performance of armour ceramics: Influence of design and structure Ceramics International", *Volume 36, Pages 2117-2127, (2010)*.
- [2] S. Vignesh, R. Surendran, T. Sekar, and B. Rajeswari, "Ballistic impact analysis of graphene nanosheets reinforced kevlar-29", *Materials Today, 45 (2021) 788–793, (Proceedings)*. <https://doi.org/10.1016/j.matpr.2020.02.808>
- [3] J. Naveen, M. Jawaid, K.L. Goh, D.M. Reddy, C. Muthukumar, T.M. Loganathan, and K.N.G.L. Reshwanth, "Advancement in Graphene-Based Materials and Their Nacre Inspired Composites for Armour Applications – A Review". *J. Nanomaterials, 11(5), 1239, 2021*. doi:10.3390/nano11051239
- [4] A. Ali, R. Adawiyah, K. Rassiah, W.K Ng, F. Arifin, F. Othman, S.H. Muhammad, M.K. Faidzi, M.F. Abdullah, and A.M.M.H. Megat, "Ballistic impact properties of woven bamboo- woven E-glass- unsaturated polyester hybrid composites", *Defence Technology, 2018*. doi:10.1016/j.dt.2018.09.001.
- [5] S. Sharma, S.R. Dhakate, A. Majumdar, and B.P. Singh, "Improved static and dynamic mechanical properties of multiscale bucky paper interleaved Kevlar fiber composites". *J. Carbon 152 631–642, (2019)*.
- [6] S. Riaan, and A. Sarp, "Experimental study of bullet-proofing capabilities of Kevlar, of different weights and number of layers, with 9 mm projectiles", *15 (2) (2019) 186–192. (Defence Technol.)*
- [7] U. Heisserer and H. Van der Werff, "The relation between Dyneema fiber properties and ballistic protection performance of its fiber composites", *vol. 3, no. 3, pp. 242–246, 2012. (Conference Proceedings)*
- [8] A. Emamverdian, Y. Ding, F. Ranaei, and Z. Ahmad, "Application of Bamboo Plants in Nine Aspects", 1–9, *The Scientific World J., 2020*, doi:10.1155/2020/7284203
- [9] R.B. Ashok, C.V. Srinivasa, and B. Basavaraju, "Dynamic mechanical properties of natural fiber composites—a review", *volume 2, pages. 586–607, 2019. (Advanced Composites and Hybrid Materials)*
- [10] I. Gago, M. del Río, J. Carretero, G. León, I. Ibarra, and B. Miguel, "Graphene-based nanocomposites with improved mechanical and ballistic protection properties", *Advanced Materials for Defense. Springer Proceedings in Materials, volume 4, Springer, Cham, 2020. (Conference Proceedings)*
- [11] Z. Parnia, R. Zahari, M.T.H. Sultan, and D.L.A.H.A. Majid, "Extraction and Preparation of Bamboo Fibre-Reinforced Composites", *J. Materials & Design (1980-2015) 63:820-828, Nov. 2014*. DOI:10.1016/j.matdes.2014.06.058
- [12] B.A. Harish, B.M. Hanumesh, T.M. Siddesh, and B.K. Siddhalinges, "An Experimental Investigation on Partial Replacement of Cement by Glass Powder in Concrete", *International Research J. of Engineering and Technology, vol. 3, issue 10, pp. 12-21, 2016*.
- [13] G.W. Sullivan, M.E. Wicks, and P.C. Koelling, "Engineering Economy-Textbooks", *Sixteenth Edition. Published by Pearson Higher Education, Permissions Department, One Lake Street, Upper Saddle River, NJ 07458, 2015. (ISBN-13: 978-0-13-343927-4)*.
- [14] S.A. Basha, G.K. Raja, and S. Jebaraj, "A review of biodiesel production, combustion, emissions and performance". *J. of Renewable Sustainable Energy, 13: 1628–34, 2009*.
- [15] M.Y. Shen, W.Y. Liao, T.Q. Wang, and W.M. Lai, "Characteristics and Mechanical Properties of Graphene Nanoplatelets-Reinforced Epoxy Nanocomposites: Comparison of Different Dispersal Mechanisms", *J. Sustainability 13, 1788, 2021*. <https://doi.org/10.3390/su13041788>
- [16] S. Stankovich, D.A. Dikin, G.H.B. Dommett, K.M. Kohlhaas, E.J. Zimney, E.A. Stach, D. Richard, Piner, S.T. Nguyen, and R.S. Ruoff, "Graphene-based composite materials", *J. Nature. 442: Pp. 282–286, 2006*.
- [17] M. Kerma, "CBN Update", Edition.cdr. cbn.gov.ng. vol.7 No.5, May 2025. ISSN No: 2695-2394. <https://www.cbn.gov.ng/Out/2025/CCD>. (May Report 2025 edition)